Research Square

Preprints are preliminary reports that have not undergone peer review.
They should not be considered conclusive, used to inform clinical practice,
or referenced by the media as validated information.

# A novel mouse model of idiopathic pulmonary fibrosis established by in situ lung injection of bleomycin

**Guoqiang Liao**
Chengdu Chipscreen Pharmaceutical CORP
**Lei Qu**
Sichuan Agricultural University
**Qihui Luo**
Sichuan Agricultural University
**Ting Fan**
Chengdu Chipscreen Pharmaceutical CORP
**Shengjian Huang**
Chengdu Chipscreen Pharmaceutical CORP
**Xuhua Mao**
Chengdu Chipscreen Pharmaceutical CORP
**Beizhong Chen**
Chengdu Chipscreen Pharmaceutical CORP
**Zhengli Chen**
chzhli75@sicau.edu.cn

Sichuan Agricultural University

**Research Article**

**Keywords:** IPF, Mouse model, BLM, in situ injection, Nintedanib

**Posted Date:** August 6th, 2026

**DOI:** https://doi.org/10.21203/rs.3.rs-10440054/v1

**License:** This work is licensed under a Creative Commons Attribution 4.0 International License.
Read Full License

**Additional Declarations:** No competing interests reported.

# Abstract

### Background

Drug induction, mechanical stimulation and gene editing are common strategies for idiopathic pulmonary fibrosis (IPF) mouse models, with bleomycin (BLM) the most widely used inducer. Classic intratracheal BLM instillation suffers from difficult operation and inconsistent lesions. This study established a novel left-lung in situ BLM injection model and evaluated nintedanib efficacy to resolve these drawbacks.

### Methods

Tracer distribution was compared between intratracheal and in situ injection. Animal survival, body weight and pathological indexes were measured for model comparison. We set sham, BLM model and nintedanib treatment groups. Histological staining and qRT-PCR detected lung injury; Student's t-test was adopted for statistics ($p < 0.05$).

### Results

In situ injection achieved uniform left-lung agent distribution. It induced typical IPF phenotypes (weight loss, inflammation, collagen deposition) with easier operation and higher animal survival than intratracheal instillation. Nintedanib notably alleviated lung fibrotic lesions in this new model.

### Conclusions

This in situ BLM injection method is simple to master after short training, stable and suitable for routine preclinical IPF modeling and antifibrotic drug screening.


# 1 Introduction

Idiopathic pulmonary fibrosis (IPF), a progressive and fatal interstitial lung disease, exhibits a median post-diagnosis survival of 3–5 years[1],surpassing the mortality rates of many malignancies. The disease pathogenesis involves aberrant extracellular matrix remodeling, manifested histologically by fibroblast foci proliferation, architectural distortion, and advanced honeycombing – pathological hallmarks that culminate in irreversible pulmonary functional decline. This cancer-like mortality profile has prompted reclassification of IPF as a "fibrotic malignancy" in recent consensus statements. Despite substantial advances in elucidating disease mechanisms, including dysregulated epithelial-mesenchymal transition and TGF-β signaling pathways, therapeutic options remain severely constrained. To date, only two antifibrotic agents – Nintedanib (a tyrosine kinase inhibitor) and Pirfenidone (an anti-inflammatory compound) – have been conditionally recommended by international guidelines (ATS/ERS/JRS/ALAT 2022), demonstrating modest efficacy in slowing disease progression.

Animal models of IPF play a crucial role for studying pathological mechanisms, evaluating new therapeutic approaches, and tracking disease progression. A series of clinically valuable drugs have been obtained through animal model screening and evaluation[2–4]. There are various methods for constructing animal models of IPF, none of them shows perfect totally. Common modeling methods include induction by drugs such as bleomycin and cyclophosphamide, induction by minerals such as silica and asbestos[5–7]. Among these modeling methods, bleomycin has been widely used for its rapid induction of the disease process. Bleomycin is a class of water-soluble alkaline glycopeptide antibiotic mixtures consisting mainly of bleomycin A2 (55–70%) and B2 (25–32%). It is widely used in squamous carcinomas of the head and neck, esophagus, and genitalia, as well as in Hodgkin's disease lymphomas. In clinical use, it has been found to cause nonspecific pneumonia to pulmonary fibrosis and the risk is positively correlated with age and dose. The combination of bleomycin and vincristine can even cause rapid death from pulmonary fibrosis.

Over the past few decades, lung damage by bleomycin represents a typical feature of IPF, and it has become the most commonly reagent for IPF modeling. Bleomycin induces lung injury and lung repair by a variety of methods, including intratracheal drip, intraperitoneal injection, subcutaneous injection, intravenous injection, and osmotic pumps. Among of them, tracheal drip can make bleomycin more rapid and directly contact with lung tissue, it has been used by many researchers. Bleomycin mediates damage to alveolar epithelial cells and vascular endothelial cells in lung tissue through multiple pathways, including oxidative stress[8], inflammatory response[9], activation of the coagulation cascade[10, 11], and disruption of the balance between cell proliferation and apoptosis[12], which initiates the process of repairing damage to the lung tissue, and is considered to be a key initiating step in lung fibrosis. Sustained injury factors activate fibroblasts to transform into extracellular matrix-producing myofibroblasts. Excessive deposition of collagen and other ECM components secreted by the myofibroblasts leads to alterations in tissue structure. The entire repair process is further deranged by the interference of irritating factors, ultimately leading to structural changes and scarring of the lung tissue and severely compromising lung function.

In the 1970s, the systemic safety of bleomycin in dogs was studied by R W Fleischman et al[13]. Ten dogs injected intravenously with different doses (5, 2.5, 1.25, and 0.625 mg/kg) of bleomycin developed varying degrees of interstitial pneumonitis and pulmonary fibrosis. Another toxicology study in mice injected intraperitoneally with bleomycin solution (0.1 mg/kg) twice weekly was shown to result in very high lung lesions (Perivascular edema and cell infiltrate and Fibrosis) [14]. The data from early toxicology studies provided a basis for the induction of IPF by bleomycin. Subsequently, investigators developed animal models of IPF in several species (mice, rats, guinea pigs, hamsters, dogs and primates) [15, 16] by bleomycin. Mice have become the most commonly used animals due to their wide availability, among of them, C57BL/6J mice exhibit higher sensitivity to bleomycin.[17]

Different laboratories have developed a variety of modeling methods through using different combinations of bleomycin doses and induction techniques. Intraperitoneal injection can be used for

induction with a dose of 20–50 mg/kg, while intravenous injection (10–20 mg/kg) and intratracheal instillation (3–5 mg/kg) can only accept lower doses[18]. In another study, researchers used the method of intratracheally injecting 0.04 units of bleomycin every other week for a total of 8 injections to obtain a chronic injury model[19]. Reviewing these modeling methods, mortality has always been an inevitable fact. During the single-dose modeling process, sometimes the mortality rate of animals reached 50%[20], and there is also a 33.3% mortality rate with long-term induction at a low dose[19]. At the same time, after administering bleomycin through different methods, the distribution of bleomycin in the lung tissue of the model animals always has a great deal of randomness[21, 22], which severely limits the application of the model. Therefore, we provided a new modeling method, which is the in situ injection of bleomycin into the lung tissue, and evaluated the therapeutic effect of Nintedanib in this model. Our results confirm that the in situ model significantly improved the survival of animals and the uneven distribution of bleomycin in the lungs. The potential of this model can provide strong support for drug screening.

# 2 Materials and Methods

**2.1 Materials**: The male C57BL/6J used in the experiment were provided by Sichuan Vital River Laboratory Animal Technology Co., Ltd. (Chengdu, China). All animal experiments were operated according to the guidelines for the care and supervised by Chengdu Chipscreen Pharmaceutical CORP., Ltd. Council (Chengdu, China). All animals were housed in a facility with temperature of 20–26°C, humidity of 40%–70%, 12/12 h light/dark cycle, free access to food and water. Bleomycin was purchased from Hanhui Pharmaceuticals Co., Ltd. (Zhejiang, China). Gene expression assay kit purchased from Takara Biomedical Technology (Beijing) Co., Ltd. (RR820A, Beijing,China). The primers were obtained from the Sangon Biotech (Shanghai) Co., Ltd. (Shanghai, China). Hematoxylin-Eosin (HE) Stain Kit, Masson's Trichrome Stain Kit and HYP kit were purchased from Beijing Solarbio life sciences. (G1120, G1340 and BC0250, Beijing, China). Isoflurane for continuous anesthesia during surgery provided by RWD Life Science Co., Ltd. (R510-22-10, Shenzhen, China). Nintedanib was purchased from MCE china. (HY-50904, Shanghai, China). Isoflurane (R510-22-10, RWD Life Science Co., Ltd., Shenzhen, China) was used for inhalation anesthesia during surgical operation. Mice were induced with 3% isoflurane and maintained under 1.5% isoflurane with oxygen supply to ensure full unconsciousness throughout surgery and reduce surgical pain.

**2.2 Bleomycin induces IPF**: The animal's left side rib coat was removed one day in advance. After the animal was anesthetized, the skin on the left side of the rib cage was applied with iodophor, and the pulsating lung was visible by cutting about 1 cm of skin and muscle. A syringe aspirated 50μL of bleomycin solution, then punctured the left lung from between the ribs. After completing the injection, the muscle and skin were quickly sutured, then penicillin was applied to the wound.

**2.3 Pharmacodynamic study**: After one week of modeling, the animals were randomly divided into three groups based on body weight: Sham group (surgery only, oral purified water during the treatment period, n = 5), Model group (6 mg/kg bleomycin solution for modeling, oral purified water during the treatment

period, n = 12), Nintedanib group (6 mg/kg bleomycin for modeling, and 60 mg/kg Nintedanib solution for oral administration during the treatment period, n = 12)

**2.4 qRT-PCR**: Fresh lung tissue was extracted and ground with trizol, then chloroform was added to separate the supernatant, isopropanol was supplied for precipitation. 75% alcohol was used to wash the precipitate, and dry it to obtain the RNA. Reverse transcription and Quantitative Real-time PCR were completed according to the standard operating procedures of the kit, and primers listed in Table1. The relative expression of each gene was calculated by the ΔCT.

**2.5 Histopathological studies**: H&E staining: H&E staining was applied to determine scores of lungs inflammation. The 4 μm paraffin section of each sample was used to assess lungs histology following the standard protocol. Paraffin sections were deparaffinized and placed in hematoxylin staining solution for 3–8 minutes before using tap water to elute excess hematoxylin. Sections were stained in eosin stain about 1–3 minutes and rinsed with tap water. Finally, the slices are dehydrated and sealed. Lung inflammation scores rang 0–4(Inflammatory cell infiltrate: 0–4 for none to very severe, Widened alveolar septa: 0–4 for none to very severe, Total score 8).

Table 1
Sequences of primers for Quantitative Real-time PCR analysis.

| Gene | Forward (5'-3') | Reverse (5'-3') |
|---|---|---|
| TGF-β | tct gca ttg cac tta tgc tga | aaa ggg cga tct agt gat gga |
| TNF-α | ccc tca cac tca gat cat ctt ct | gct acg acg tgg gct aca g |
| IL-6 | tag tcc ttc cta ccc caa ttt cc | ttg gtc ctt agc cac tcc ttc |
| IL-1β | gca act gtt cct gaa ctc aac | atc ttt tgg ggt ccg tca act |
| α-SMA | gtc cca gac atc agg gag taa | tcg gat act tca gcg tca gga |
| Col1a1 | gct cct ctt agg ggc cac t | cca cgt ctc acc att ggg g |
| GAPDH | agg tcg gtg tga acg gat ttg | tgt aga cca tgt agt tga ggt ca |

Masson staining: Masson staining was applied to determine lungs fibrosis. The 4 μm paraffin section of each sample was used in this study and followed the standard procedure. The sections were stained with hematoxylin staining solution for 5–10 minutes and then washed, followed by staining with Ponceau S acid fuchsin stain around 5–10 minutes. The sections were treated with 1% phosphomolybdic acid and aniline blue solution, and finally dehydrated stepwise in alcohol and sealed. Pulmonary fibrosis score according to the Ashcroft scoring system as normal lung tissue to fibrotic foci appear throughout the area (rang: 0–8)

**2.6 Statistical analysis**: All data from the experiment were counted using GraphPad Prism 8.0 software and expressed as mean ± standard deviation (SD). Student's t test was used to compare means between two groups.$p < 0.05$ was considered statistically significant.

# 3 Results

## 3.1 In situ injection of bleomycin provides superior dispersion in the lungs

We injected different volumes of indicator into the left lung to simulate the distribution of bleomycin in the lungs. After the injection was completed, the animals were euthanized and lung tissues were harvested. The results of the tissue sampling showed that 100μL volume of the indicator filled the entire left lung and some of the solution spread to the right lung (Fig. 1A), while 50μL volume evenly filled the left lung (Fig. 1B). At the same time, we compared the distribution of the indicator in the lungs after 50μL of the indicator was injected through the trachea and found that the indicator was mainly concentrated at the bifurcation of the main bronchus, and the distribution of the indicator in each lung lobe was randomly scattered (Fig. 1C). After the injection operation, all experimental mice were euthanized at predetermined experimental endpoints. Briefly, mice were first anesthetized via inhalation of 3% isoflurane until complete loss of pain reflex and consciousness. Subsequently, cervical dislocation was performed as the primary euthanasia method. Cervical dislocation was selected in accordance with institutional animal welfare standards, which can rapidly induce brain death and minimize sustained suffering of experimental animals. No injectable euthanasia agents were used in this study. After euthanasia, complete lung tissue was immediately separated for subsequent observation, staining and molecular detection.

## 3.2 Bleomycin rapidly induces unilateral lung injury in a dose-dependent manner

In situ injection of bleomycin demonstrated superior distribution characteristics, and we conducted a short-term study on lung injury in animals with different doses of bleomycin (Fig. 2A). We monitored the changes in body weight of the animals within a week, and the body weight of animals stimulated with different doses of bleomycin decreased (Fig. 2B). The body weight of the animals in the 2.5 mg/kg group and 5 mg/kg group recovered after about 5 days and increased rapidly, without any other obvious abnormalities. The animals in the 10 mg/kg group exhibited significant severe conditions such as disheveled fur and reduced movement. Seven days after bleomycin stimulation, the animals were euthanized. Significant areas of damage/necrosis were seen in the left lung, while the right lung appeared normal (Fig. 2C). The fibrosis scoring results also indicated significant fibrosis in the left lung, with the degree of fibrosis being dose-dependent (Fig. 2D). Significant differences were observed between the 2.5 mg/kg and 10 mg/kg groups (* $p < 0.05$), as well as between the 5 mg/kg and 10 mg/kg groups (** $p < 0.01$). Under the microscope, alveolar damage and collagen fiber deposition caused by interstitial and alveolar fibrosis were observed in the left lungs of all animal groups. At the same time, the staining results of the right lung showed no obvious damage (Fig. 2E).

## 3.3 In situ injection induces IPF symptoms similar to the traditional approach

Pre-experiments confirmed that in situ injection of bleomycin can cause unilateral lung injury, and we subsequently compared the similarities and differences between in situ and conventional intratracheal instillation modeling of IPF (Fig. 3A).The IPF model showed typical body weight changes, and we continuously monitored and found that animals of both modeling modalities showed body weight reduction after modeling, whereas the animals in the sham did not show any body weight reduction, demonstrating that surgical modeling does not affect the basal vital signs of the animals (Fig. 3B). At the same time, animals stimulated at the same dose (5 mg/kg) after in situ injection showed smaller body weight changes and faster recovery rates compared to intratracheal instillation. We calculated lung/body weight ratios and showed an increase on days 7 and 21 after bleomycin treatment compared to the sham, with a greater degree of change in lung/body weight ratios at day 21 compared to day 7 after intratracheal instillation (5 mg/kg) modeling, whereas in situ injections demonstrated a more stable result (Fig. 3C, D). On day 21 we examined the hydroxyproline (HYP) quantification in the right posterior lobe of the lungs, and the results showed that the 2.5 and 5 mg/kg groups exhibited an elevated trend in HYP, whereas the 10 mg/kg and intratracheal instillation groups exhibited lower HYP levels (Fig. 3E).

Pathohistological staining of the model group at low magnification revealed fibrotic areas distributed in the subpleural and paraspinal areas, which were mainly composed of dense collagen fibers accompanied by scattered fibroblasts and myofibroblasts. In addition, the foveal changes appeared microscopically as fibrotic cystic cavities formed after the proliferation of fine bronchial epithelium, containing mucus and inflammatory cells. The alveolar structure was disorganized and irregular, with marked thickening of the alveolar walls and a large infiltration of lymphocytes and macrophages. Among them, only the low-dose bleomycin group (2.5 mg/kg) had fewer lung solid lesions at day 7, while the rest of the groups all showed severe lung solid lesions at different times, and the lung function was severely damaged (Fig. 3F,G). The experimental results further indicated that in situ injection of bleomycin was a feasible modality for modeling, and by combining the performance of each concentration of bleomycin, we concluded that 5 mg/kg was suitable for in situ injection.

## 3.4 Progression of IPF induced by in situ injection of bleomycin

Next, we investigated the changes in the lungs at different periods after bleomycin stimulation (Fig. 4A). Although the 10 mg/kg dose induced more extensive fibrosis, it also caused severe deterioration in animal welfare, including reduced mobility, ruffled fur, and significant weight loss (Fig. 2B-D). Therefore, we selected the 5 mg/kg dose for subsequent longitudinal studies, as it provided robust and reproducible fibrotic lesions while maintaining acceptable animal welfare standards — a dose range (3–6 mg/kg) commonly used in previous intratracheal instillation studies [5, 18].After stimulation with 5 mg/kg, the body weight of the animals decreased in the short term and recovered within a week (Fig. 4B). After sacrificing the animals, the lung tissues showed significant damage compared to the sham group, with the left lung being more severely affected than the right lung. On the 21st day, some animals exhibited atrophy and hardening of the left lung without elasticity (Fig. 4C).

Histopathology is a test recommended by numerous international guidelines, HE staining showed that the lung tissue structure of the sham-operated mice was intact, while the model mice presented severe pneumonia and inflammatory cells on 7–14 days. We observed pulmonary alveoli structure was significantly altered, with a large number of neutrophils infiltrating the alveolar spaces and interstitium, some alveolar spaces were destroyed or disappeared, and there was proliferation of fibroblasts and capillaries in the lung septa. On the 14th-21st day, pulmonary fibrosis begins to form, macrophages, neutrophils and other inflammatory cells show a tendency to decrease, at this time there is an increase in fibroblasts, and the alveolar septum is significantly thickened and accompanied by collagen deposition. The results on the 21st day showed that most mice developed diffuse pulmonary interstitial fibrosis, with the interstitium replaced by collagen fibers and fibroblasts, destruction of the alveolar walls, formation of lung bullae, but inflammatory cell infiltration was still visible. On the 28th day, the inflammatory cells decreased to a low level, and the degree of fibrosis also began to regress (Fig. 4D). The scores for inflammation and fibrosis also indicated that the damage after in situ injection of bleomycin mainly occurred in the first 3 weeks, and a self-limiting condition began to appear in the fourth week (Fig. 4E, F).

At the same time, we also detected the expression of genes related to inflammation and fibrosis. Bleomycin stimulation immediately promoted the high expression of genes such as IL-1β, α-SMA, and COL1a1 in the left lung, a process that lasted for about 2 weeks. However, the high expression of related genes in the right lung occurred one week later, and by the fourth week, the expression of related genes gradually returned to normal in both lungs (Fig. 4G-J).

## 3.5 Nintedanib significantly ameliorated bleomycin-induced inflammation and fibrosis

By directly administering bleomycin into the lungs, we successfully induced IPF models and subsequently evaluated the therapeutic efficacy of Nintedanib (Fig. 5A). Consistent with previous experiments, the model animals exhibited a decline in body weight, whereas the sham group showed no significant changes. A dose of 60 mg/kg Nintedanib did not induce systemic safety risks in the animals (Fig. 5B). After two weeks of Nintedanib treatment, the animals were euthanized, and lung tissues were harvested to calculate the lung-to-body weight ratio. The model group demonstrated a significant increase in this index compared to controls, with marked improvement observed following Nintedanib therapy (Fig. 5C).

Histopathological examination is important for the assessment of the severity and progression of IPF, as well as to monitor the efficacy of treatment during the course of treatment, we chose HE and MASSON staining to assess the degree of inflammatory cell infiltration and fibrosis after Nintedanib treatment. We observed that the model showed typical interstitial pneumonia, and multiple inflammatory foci could be observed in the model under the microscope, and there was a reduction in the inflammatory infiltration after treatment. At the same time, the model animals showed unevenly distributed foci of dense fibrosis, in which a large number of light-colored fibroblasts with lung structural remodeling could be observed,

which was also improved after Nintedanib treatment (Fig. 5D). Scoring systems assessing the model group of animals mostly showed higher scores for inflammatory infiltrates and collagen fiber deposition, whereas treatment significantly reduced the scores (Fig. 5E, F). Gene expression is often highly correlated with pathogenesis, and in the present study we have demonstrated that a variety of inflammatory and fibrotic genes are highly expressed by bleomycin stimulation, and after drug intervention we found that the expression of TNF-α and IL-6 was regulated to a greater extent and gradually returned to normal levels. Among the genes associated with fibrosis, COL1a1 showed sensitivity to treatment with Nintedanib (Fig. 5G).

# 4 Discussion

This study devised a novel IPF modeling approach that surgically allows the operator to see the complete lung morphology and subsequently visualize the introduction of bleomycin. in situ injection of bleomycin was performed in a way that was less harmful to the animal and less difficult to perform. Subsequently, a variety of tests have shown that the lungs were damaged by bleomycin and that this approach mimicked the course of clinical IPF to some extent. The results of this study suggest that the extension of this modeling approach will provide a new way of evaluating drug screening for the treatment of IPF.

This study compared the differences between in situ and conventional modeling approaches from phenotype to mechanism. Significant physiological abnormalities (decreased activity, disheveled hair) were seen in the animals within a week of receiving bleomycin, which visually reflected the damage that had occurred in the lungs. Pathological sections taken at different times after multiple doses of bleomycin visualized the actual lung damage, with infiltrating inflammatory cells and deposited collagen fibers reflecting the severity of structural and functional damage. Differences between the two modeling modalities could be observed under the microscope, with in situ unilateral injections showing inflammation and diffuse distribution of fibers, and intratracheal instillations focusing more on the trachea, and indicators showed that the damage from intratracheal instillations of 5 mg/kg bleomycin was equivalent to that from in situ injections of 10 mg/kg (Fig. 3C-G), which appeared to explain why tracheally injected animals tended to show worse physiological status.

Intratracheal instillation of bleomycin is the most commonly used method for establishing IPF models. and we have successfully induced IPF symptoms in animals using this method. However, due to the physiological structure of mice, which has a long and narrow pharynx and a small tracheal opening that is not easy to be observed, bleomycin can easily be mistakenly injected into the esophagus, resulting in reduced stimulation or failure of stimulation. At the same time, this operation must be performed under deep anesthesia, at which time the breathing of the animal becomes shallow, and the introduction of bleomycin can easily cause asphyxiation and lead to instantaneous death of the animal, which has been mentioned in a previous study[20], which is against the welfare of experimental animals. intratracheal instillation of bleomycin requires rapid and accurate completion by the experimenter in conjunction with specialized equipment to minimize injury to the animal. The experimental design of in situ injection of

bleomycin in the left lung to induce IPF was derived from an in situ lung cancer model[23], and we changed the object of injection from cells to bleomycin, and during the modeling process, we strictly adhered to the ethical and safety guidelines in lung cancer injections, and used isoflurane anesthesia to alleviate the pain of the animals, so that the surgery and the injection of bleomycin could be completed in a short period of time. No obvious abnormalities were observed in all animals after surgery, and body weight monitoring data showed that unilateral lung injury was less likely to lead to systemic abnormalities, whereas intratracheal instillations often led to bilateral lung injury, causing severe weight loss and even death. in situ injection requires the researcher to accurately localize the lung (6th-10th intercostal space) and bluntly separate the skin before completing the injection. The success rate of introducing bleomycin using in situ injection by trained operators was significantly higher than intratracheal instillation. In summary, we concluded that intratracheal instillation of bleomycin requires a high level of experimental technique from the operator, and that in situ injection is more suitable for researchers as a simple and efficient way of operation.

The right lung also showed slight damage after in situ injection as seen during lung tissue sampling, which was inconsistent with the stain tracing. We hypothesized that the lungs extruded bleomycin solution into the right lung during contraction, which caused expression of relevant genes and slight phenotypic damage. No structural damage to the right lung was observed after histopathologic examination, suggesting a role for lung self-repair. In contrast, most of the lungs modeled by intratracheal instillation failed to repair themselves, suggesting that these two modeling modalities may represent early IPF and late IPF.The structural and functional integrity of the right lungs remained intact after in situ injection, and the lung stem cells in the right lungs were less damaged by bleomycin, and they were able to differentiate into different types of mature lung cells to complete the regeneration of alveolar cells and reconstruction of the epithelial barrier. It was shown that after SARS-CoV-2 infection, KRT5/P63 double-positive as well as TM4SF1-positive lung stem cell cells could repair broken alveolar barrier cells, thus avoiding infiltration of broken alveolar cells by immune cells[24]. In another study bleomycin intratracheal instillation followed by administration of lung stem cells significantly improved lung health[25], which indicates both the greater damage to lung stem cells in the bleomycin intratracheal instillation model and the damage repairing effect of lung stem cells on the lung. In addition to this, the lungs are the main site of gas exchange in the body, and severe pulmonary dysfunction in both lungs is very likely to cause multi-organ failure, a physiological imbalance that is difficult to reverse by drugs, and the other lung can functionally compensate to maintain normal physiological activities after single-lung injury. In summary, we believe that the in situ injection model can better predict the treatment outcome of early IPF patients, while the intratracheal instillation model is more biased towards evaluating the later treatment of IPF.

# Abbreviations

IPF
Idiopathic pulmonary fibrosis

BLM
Bleomycin
HYP
Hydroxyproline
α-SMA
Alpha-smooth muscle actin
COL1a1
Collagen type I alpha 1 chain
TGF-β
Transforming growth factor-β
TNF-α
Tumor necrosis factor-α
IL-1β
Interleukin-1β
IL-6
Interleukin-6
qRT-PCR
Quantitative real-time polymerase chain reaction
HE
Hematoxylin-Eosin.

## Declarations

# Ethics approval and consent to participate

All animal experiments were reviewed and approved by the Institutional Animal Care and Use Committee of Sichuan Agricultural University (20240112). All animal operation procedures complied with national laboratory animal welfare guidelines and the animal research policies of BMC Pulmonary Medicine. No human participants or human tissues were involved in this study.

### Consent for publication

Not applicable. This study only involves laboratory mice, and no individual human data, images or case records are included in the manuscript.

# Competing Interests

The authors declare that they have no competing interests.

# Funding

The authors declare that no funds, grants, or other financial support were received during the preparation of this manuscript.

# Author Contribution

GL. conceived the study and provided the modeling ideas and methods. GL. LQ. and QL. designed the experiments, analyzed the data, prepared the tables and figures, and wrote the original draft of the manuscript. SH. and TF. reviewed and edited the manuscript. GL. XM. and BC. performed the animal experiments. ZC. and BC. conducted the histopathological examinations and evaluated the results. All authors read and approved the final manuscript.

# Acknowledgements

Not applicable.

# Availability of data and materials

The datasets used and analysed during the current study are available from the corresponding author on reasonable request.

## References

1. Ley B, Collard HR, King TJ. Clinical course and prediction of survival in idiopathic pulmonary fibrosis. Am J Respir Crit Care Med. 2011;183(4):431–40.
2. Cras TDL, Korfhagen TR, Davidson C, et al. Inhibition of PI3K by PX-866 Prevents Transforming Growth Factor-α–Induced Pulmonary Fibrosis. Am J Pathol. 2010;176(2):679–86.
3. Liu H, Wu X, Gan C, et al. A novel multikinase inhibitor SKLB-YTH-60 ameliorates inflammation and fibrosis in bleomycin-induced lung fibrosis mouse models. Cell Prolif. 2021;54(7):e13081.
4. Tanner L, Single AB, Bhongir R, et al. Small-molecule-mediated OGG1 inhibition attenuates pulmonary inflammation and lung fibrosis in a murine lung fibrosis model. Nat Commun. 2023;14(1):643.
5. Liu T, De Los SF, Phan SH. The Bleomycin Model of Pulmonary Fibrosis. Methods Mol Biol. 2017;1627:27–42.
6. Dinh PC, Paudel D, Brochu H, et al. Inhalation of lung spheroid cell secretome and exosomes promotes lung repair in pulmonary fibrosis. Nat Commun. 2020;11(1):1064.

7. Naccache JM, Jouneau S, Didier M, et al. Cyclophosphamide added to glucocorticoids in acute exacerbation of idiopathic pulmonary fibrosis (EXAFIP): a randomised, double-blind, placebo-controlled, phase 3 trial. Lancet Respir Med. 2022;10(1):26–34.
8. Abidi A, Bahri S, Ben KS, et al. A comparative study of intratracheal and aerosolization instillations of bleomycin inducing experimental lung fibrosis in rat. Toxicol Mech Methods. 2019;29(2):75–85.
9. Yokoyama T, Yanagihara T, Suzuki K, et al. Depletion of club cells attenuates bleomycin-induced lung injury and fibrosis in mice. J Inflamm (Lond). 2017;14:20.
10. Chambers RC. Procoagulant signalling mechanisms in lung inflammation and fibrosis: novel opportunities for pharmacological intervention? Br J Pharmacol. 2008;153(Suppl 1):S367–78.
11. Dai C, Lin X, Qi Y, et al. Vitamin D3 improved hypoxia-induced lung injury by inhibiting the complement and coagulation cascade and autophagy pathway. BMC Pulm Med. 2024;24(1):9.
12. Vats A, Chaturvedi P. The Regenerative Power of Stem Cells: Treating Bleomycin-Induced Lung Fibrosis. Stem Cells Cloning. 2023;16:43–59.
13. Fleischman RW, Baker JR, Thompson GR, et al. Bleomycin-induced interstitial pneumonia in dogs. Thorax. 1971;26(6):675–82.
14. Adamson IY, Bowden DH. The pathogenesis of bleomycin-induced pulmonary fibrosis in mice. Am J Pathol. 1974;77(2):185–97.
15. Moore BB, Hogaboam CM. Murine models of pulmonary fibrosis. Am J Physiol Lung Cell Mol Physiol. 2008;294(2):L152–60.
16. Tashiro J, Rubio GA, Limper AH, et al. Exploring Animal Models That Resemble Idiopathic Pulmonary Fibrosis. Front Med (Lausanne). 2017;4:118.
17. Yamamoto T, Kuroda M, Nishioka K. Animal model of sclerotic skin. III: Histopathological comparison of bleomycin-induced scleroderma in various mice strains. Arch Dermatol Res. 2000;292(11):535–41.
18. Gul A, Yang F, Xie C, et al. Pulmonary fibrosis model of mice induced by different administration methods of bleomycin. BMC Pulm Med. 2023;23(1):91.
19. Degryse AL, Tanjore H, Xu XC, et al. Repetitive intratracheal bleomycin models several features of idiopathic pulmonary fibrosis. Am J Physiol Lung Cell Mol Physiol. 2010;299(4):L442–52.
20. Harrison JJ, Lazo JS. High dose continuous infusion of bleomycin in mice: a new model for drug-induced pulmonary fibrosis. J Pharmacol Exp Ther. 1987;243(3):1185–94.
21. Abidi A, Bahri S, Ben KS, et al. A comparative study of intratracheal and aerosolization instillations of bleomycin inducing experimental lung fibrosis in rat. Toxicol Mech Methods. 2019;29(2):75–85.
22. Togami K, Kanehira Y, Yumita Y, et al. Heterogenous Intrapulmonary Distribution of Aerosolized Model Compounds in Mice with Bleomycin-Induced Pulmonary Fibrosis. J Aerosol Med Pulm Drug Deliv. 2023;36(6):289–99.
23. Xu W, Yang S, Lu L, et al. Influence of lung cancer model characteristics on tumor targeting behavior of nanodrugs. J Controlled Release. 2023;354:538–53.

24. Zhao Z, Zhao Y, Zhou Y, et al. Single-cell analysis identified lung progenitor cells in COVID-19 patients. Cell Prolif. 2020;53(12):e12931.
25. Dinh PC, Paudel D, Brochu H, et al. Inhalation of lung spheroid cell secretome and exosomes promotes lung repair in pulmonary fibrosis. Nat Commun. 2020;11(1):1064.

# Figures

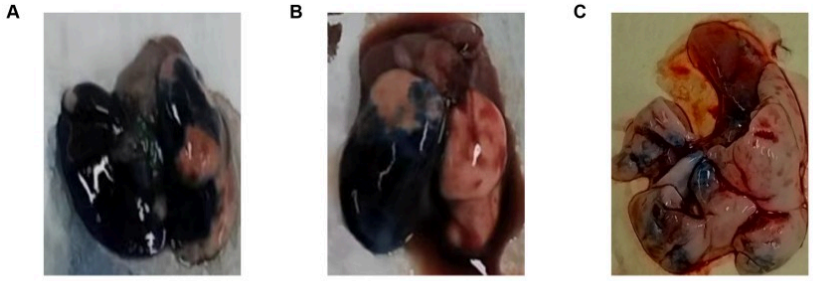



**Figure 1**

**Different ways to introduce bleomycin into the lung.** Distribution of 100μL (A) and 50μL (B) of stain in lung tissue after 30 seconds by in situ injection into the left lung. (C) Distribution of 50 microliters of stain through the trachea into the lungs and the distribution of the stain in lung tissue after 30 seconds.

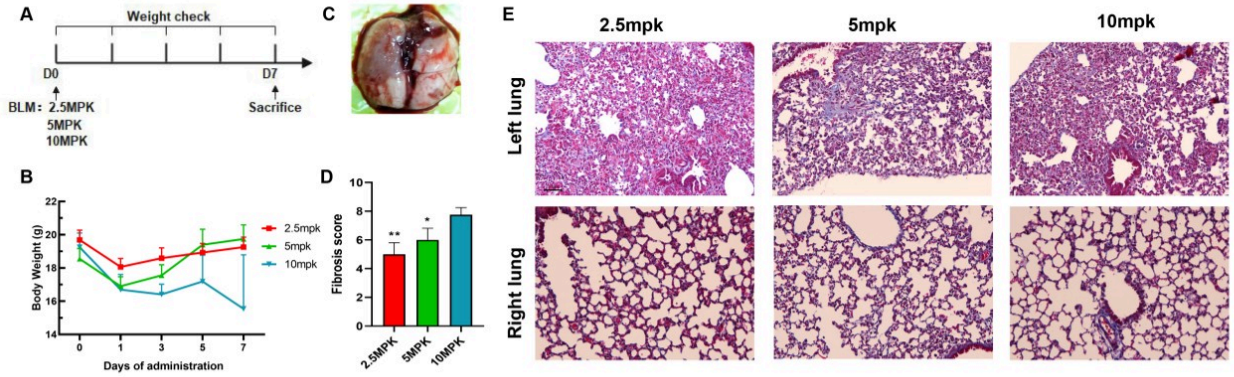
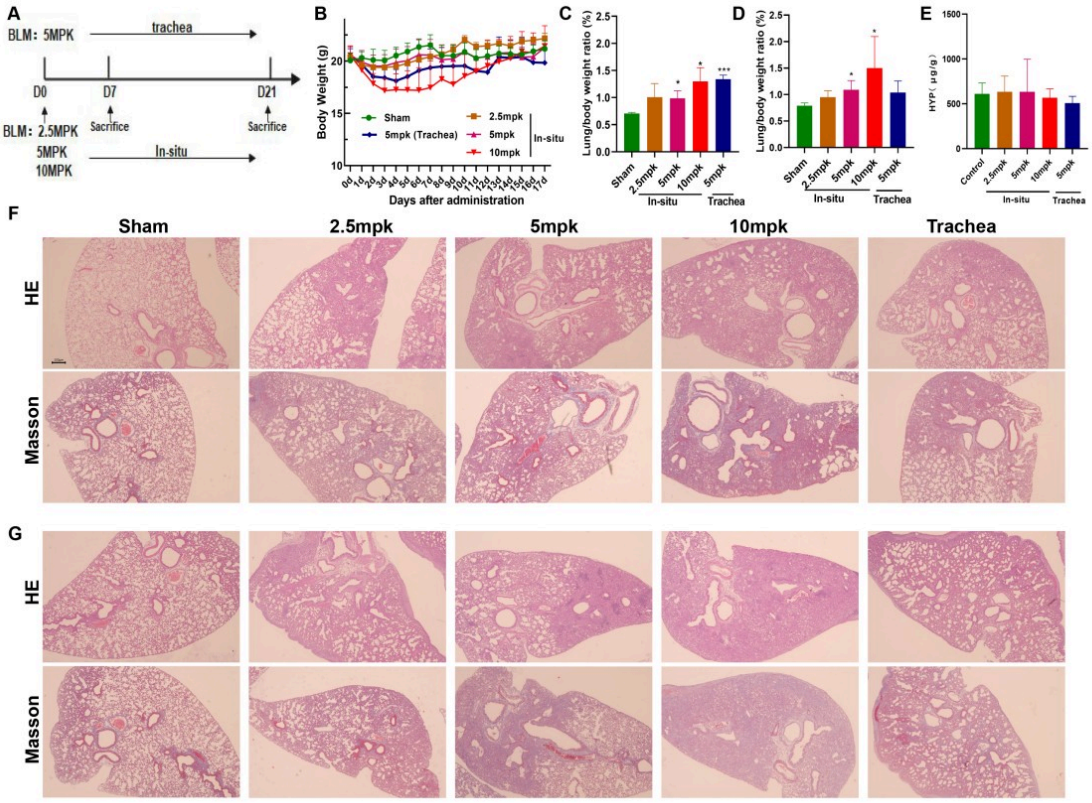


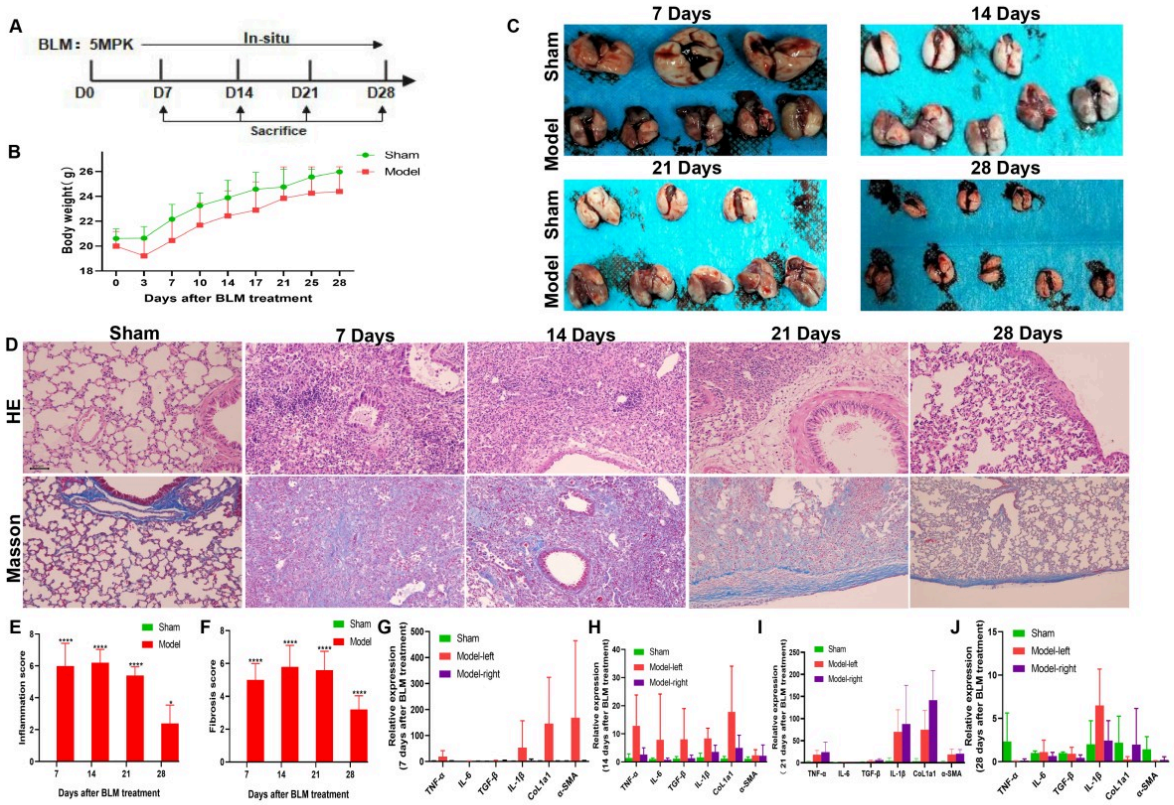

**Figure 2**

**In situ injection of bleomycin induces IPF symptoms.** (A) Schematic representation of study. (B) Weight changes during the study period (n=4). (C) Lung lesions after 5 mg/kg bleomycin injection into the left lung for 7 days. (D) Fibrosis score by Masson staining (Scale bar: 50 μm, * represents 2.5mpk and 5mpk vs. 10mpk,. * $p < 0.05$, ** $p < 0.01$). (E) Histological changes of left and right lung were assessed by Massonstaining.



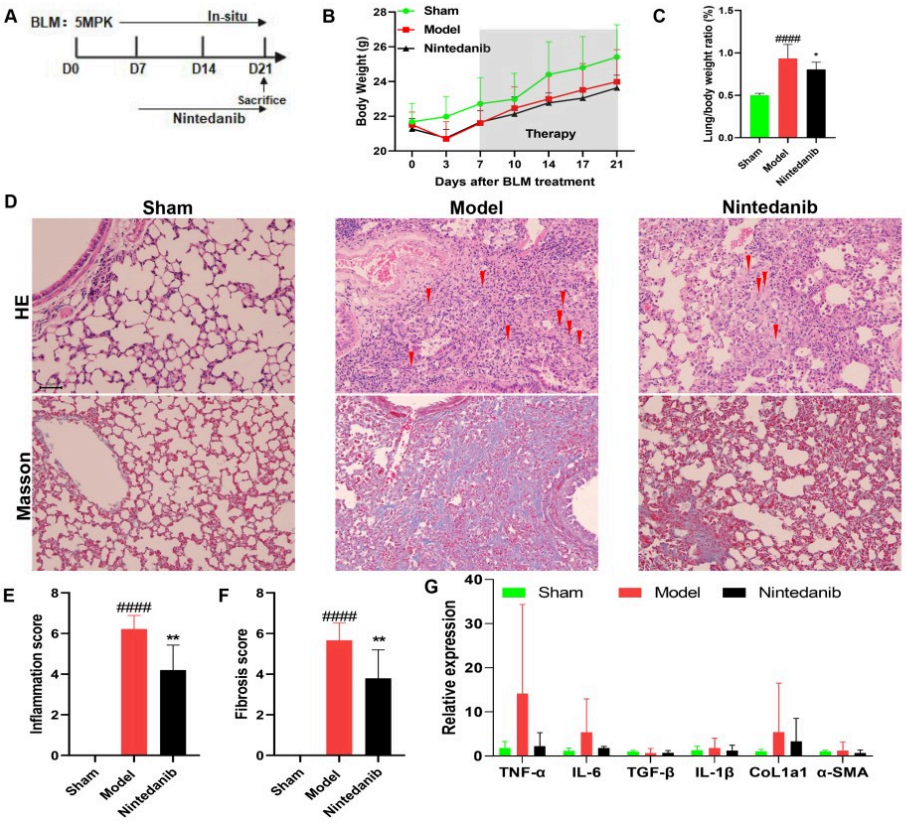

## Figure 3

**Comparison of in situ injection molding methods with conventional models.** (A) Schematic study of contrasting experiments. (B) Changes in body weight after different modalities of molding (sham: n=5, model: n=10). Lung/body weight ratios of animals after 7 days (C) 21 days (D) of bleomycin stimulation (* represents models vs. Sham, * $p < 0.05$, *** $p < 0.001$). (E) HYP content after 21 days of different molding treatments. Inflammatory infiltrates and fibrotic deposits were assessed by H□E and Masson staining at 7 days (F) and 21 days (G) (Scale bar: 200 μm).




## Figure 4

**Symptoms of IPF at different times after in situ injection of 5 mg/kg bleomycin.** (A) Schematic diagram of the experiment studied. (B) Changes in body weight of animals over 28 days (sham: n=3,model: n=5). (C) Anatomical drawings of the lungs of animals at different periods. (D) Evaluation of left pneumonic infiltration and collagen deposition at different times byHE and Masson staining (Scale bar: 50 μm). Scoring of inflammation (E) and fibrosis (F) by histopathologic examination (* represents models vs. Sham, * $p < 0.05$, **** $p < 0.0001$). Expression of inflammatory and fibrotic genes after Bleomycin Stimulation 7 (G), 14 (H), 21 (I), and 28 days (J).




## Figure 5

**Evaluation of Nintedanib in the in situ mouse model.** (A) The experimental design of Nintedanib efficacy. (B) Changes in body weight of animals during modeling and treatment (n=10). (C) Lung/body weight ratio after 2 weeks of treatment (* represents treatment vs. model, # represents model vs. Sham, * $p < 0.05$, #### $p < 0.0001$ ). (D) HE and Masson stains to assess histopathologic changes (Scale bar: 50 μm, Fibroblasts are indicated by the arrows). Scoring of inflammation (E) and fibrosis (F) by histopathologic staining (* represents treatment vs. model, # represents model vs. Sham, ** $p < 0.01$, #### $p < 0.0001$ ). (G) Expression of inflammatory and fibrotic genes after Nintedanib treatment.